J|A|C|S ARTICLES

Published on Web 12/11/2008

Light-Induced Excited Spin State Trapping: Ab Initio Study of the Physics at the Molecular Level

Nicolas Suaud,*[,†,‡] Marie-Laure Bonnet,[†,‡,§] Corentin Boilleau,[†,‡] Pierre Labèguerie,[†,‡] and Nathalie Guihéry[†,‡]

Université de Toulouse, UPS, Laboratoire de Chimie et Physique Quantiques, IRSAMC, 31062 Toulouse, France, CNRS, UMR 5626, France, and Laboratoire de Chimie, UMR 5182, Ecole normale supérieure de Lyon, 46 allée d'Italie, 69364 Lyon Cédex 07, France

Received July 18, 2008; E-mail: suaud@irsamc.ups-tlse.fr

Abstract: This paper provides a qualitative analysis of the physical content of the low-energy states of a spin-transition compound presenting a light-induced excited spin state trapping (LIESST) phenomenon, namely, $[Fe(dipyrazolpyridine)_2](BF_4)_2$, which has been studied using the wave function-based CASPT2 method. Both the nature of the low-energy states and the relative position of their potential energy wells as a function of the geometry are rationalized from the analysis of the different wave functions. It is shown that the light-induced spin transition occurring in such systems could follow several pathways involving different excited spin states. In an ideal octahedral geometry, the interconversion from the excited singlet state to the triplet of lower energy, which is usually seen as an intermediate state in the LIESST mechanism, is quite unlikely since there is no crossing between the potential energy curves of these two states. On the contrary, in lower-symmetry complexes, the geometrical distortion of the coordination sphere due to ligand constraints is responsible for the occurrence of a crossing between these two states in the Franck−Condon region, leading to a possible participation of this triplet state in the LIESST mechanism. In the reverse LIESST process, a crossing between the potential energy curves of another triplet state and the excited quintet state occurs in the Franck−Condon region as well.

1. Introduction

The possible use of spin-transition compounds as switchable systems in techological devices has motivated both experimental and theoretical fundamental research on these compounds. While several arguments attribute the macroscopic bistability property to cooperative effects,[1] the understanding of this property from a microscopic point of view is still based on molecular bistability, i.e., on the existence of two wells in the potential energy surface (PES) associated with low-spin (LS) and high spin (HS) ground states having different equilibrium geometrical structures. When the spin transition may be photoinduced, as in light-induced excited spin state trapping (LIESST) compounds,[2] a mechanism involving several excited spin states has been proposed[3] in order to rationalize the observed low-temperature transition. For a d^6 metal electronic occupation, the corresponding pathway goes from the LS singlet ground state first to an excited singlet, then proceeds to an intermediate triplet, and finally ends in the HS quintet state. A similar mechanism for the reverse LIESST mechanism has also been proposed.[4] It consists of a first excitation from the HS quintet ground state to an excited quintet state. Next, the system relaxes to an intermediate triplet state through an interconversion mechanism before coming back to the LS singlet ground state. In order to validate such mechanisms, dynamical studies are required. In the simplest of the adiabatic approaches, the PESs of the different states as well as the spin−orbit couplings at the crossings between these states should be calculated. Several methods could then be used in order to explore both the LIESST and reverse LIESST mechanisms dynamically. Because of the large number of degrees of freedom in real compounds, which usually involve quite large ligands, such an ab initio study simply appears to be nontractable. Following the pioneering work of Bolvin,[5] the present work is an attempt to address this problem and will essentially focus on the analysis of the nature of the different states that could be involved in these mecha-

[†] Université de Toulouse.
[‡] CNRS, UMR 5626.
[§] Ecole normale supérieure de Lyon.

(1) Jeftic, J.; Hauser, A. *J. Phys. Chem. B* **1997**, *101*, 10262. Martin, J.-P.; Zarembowitch, J.; Bousseksou, A.; Dworkin, A.; Haasnoot, J. G.; Varret, F. *Inorg. Chem.* **1994**, *33*, 6325. Balde, C.; Desplanches, C.; Wattiaux, A.; Guionneau, P.; Gütlich, P.; Létard, J.-F. *Dalton Trans.* **2008**, *20*, 2702.

(2) Decurtins, S.; Gütlich, P.; Köhler, C. P.; Spiering, H.; Hauser, A. *Chem. Phys. Lett.* **1984**, *105*, 1. Decurtins, S.; Gütlich, P.; Köhler, C. P.; Spiering, H. *J. Chem. Soc., Chem. Commun.* **1985**, 430. Decurtins, S.; Gütlich, P.; Hasselbach, K. M.; Hauser, A.; Spiering, H. *Inorg. Chem.* **1985**, *24*, 2174. Gütlich, P.; Hauser, A.; Spiering, H. *Angew. Chem., Int. Ed. Engl.* **1994**, *33*, 2024. Hayami, S.; Gu, Z.; Shiro, M.; Einaga, Y.; Fujishima, A.; Sato, O. *J. Am. Chem. Soc.* **2000**, *122*, 7126. Huby, N.; Guérin, L.; Collet, E.; Toupet, L.; Ameline, J.-C.; Cailleau, H.; Roisnel, T.; Tayagaki, T.; Tanaka, K. *Phys. Rev. B* **2004**, *69*, 020101. Guérin, L.; Huby, N.; Collet, E.; Toupet, L.; Cailleau, H.; Tanaka, K. *J. Phys.: Conf. Ser.* **2005**, *21*, 136. Bonhommeau, S.; Molnár, G.; Galet, A.; Zwick, A.; Real, J. A.; McGarvey, J. J.; Bousseksou, A. *Angew. Chem., Int. Ed.* **2005**, *44*, 4069. Ould Moussa, N.; Trzop, E.; Mouri, S.; Zein, S.; Molnár, G.; Gaspar, A. B.; Collet, E.; Buron-Le, M.; Real, J. A.; Borshch, S.; Tanaka, K.; Cailleau, H.; Bousseksou, A. *Phys. Rev. B* **2007**, *75*, 054101. Mouri, S.; Ould Moussa, N.; Molnár, G.; Real, J. A.; Gaspar, A. B.; Bousseksou, A.; Tanaka, K. *Chem. Phys. Lett.* **2008**, *456*, 215.

(3) McGarvey, J. J.; Lawthers, I. *J. Chem. Soc. Chem. Commun.* **1982**, 906.

(4) Hauser, A. *Chem. Phys. Lett.* **1986**, *124*, 543.

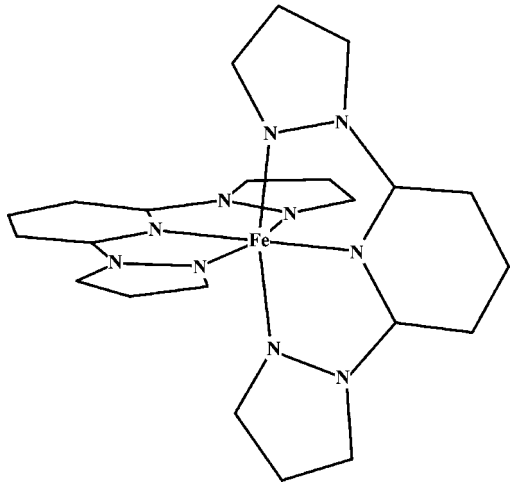

Figure 1. Crystallographic structure of the low-spin state of the $[Fe(dipyrazolpyridine)_2]^{2+}$ complex in the $[Fe(dipyrazolpyridine)_2](BF_4)_2$ compound.

nisms. Their relative energetic positions in the spectrum should provide rational arguments to orient further realistic research.

This study examines the $[Fe(dipyrazolpyridine)_2]^{2+}$ complex of the $[Fe(dipyrazolpyridine)_2](BF_4)_2$ compound (see Figure 1), which is known to present a LIESST effect below $T_{LIESST} = 81$ K. Experimental characterizations have shown that the thermal spin transition occurring at $T = 260$ K exhibits a hysteresis loop of 3 K.[6−8] Crystallographic data at different temperatures are available and show that the complex geometrical structures present a slightly distorted D_{2d} symmetry. In order to validate the methodology, the somewhat smaller and more symmetric octahedral $[Fe(NCH)_6]^{2+}$ complex has also been studied. As the HS state presents the lowest minimum,[5,9] no LIESST mechanism has been observed in this complex. Low-energy spectra of both compounds have been computed as functions of the geometry variations between two equilibrum geometries of the singlet and quintet ground states. The geometrical parameter which is the most affected by the transition is the radius of the coordination sphere around the metal ion (R_{M-L}). For this reason, potential energy curves (PECs) are usually drawn as functions of this single parameter. However, for bidentate or tridentate ligands, the constraint introduced by the coordination sphere variations induces a distortion from an ideal octahedral crystal field. This distortion differentially affects not only the Fe−N distances but also the orientation of the lone pairs of the ligands and therefore

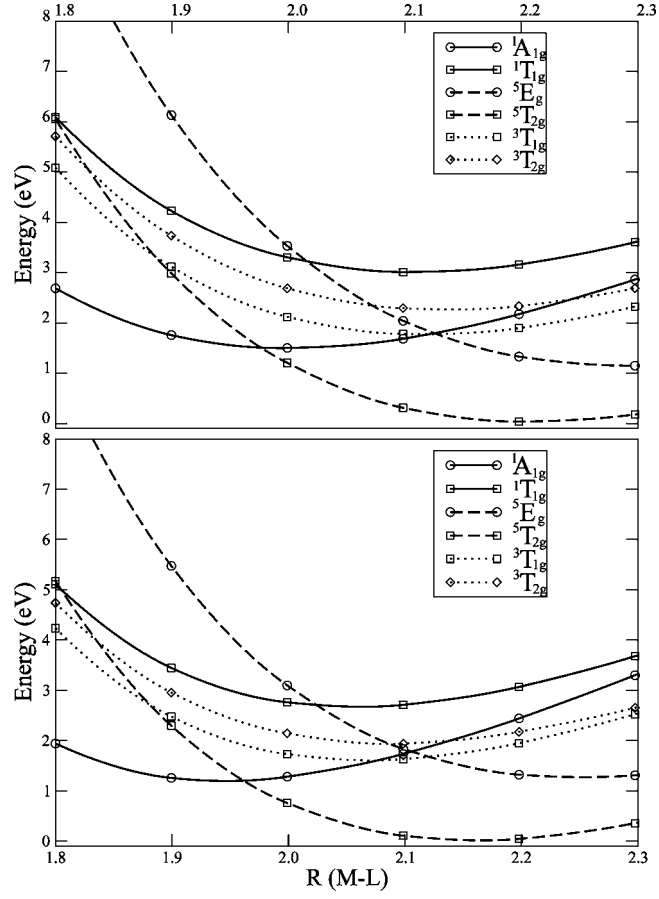

Figure 2. Potential energy curves of the low-energy states of the $[Fe(NCH)_6]^{2+}$ complex as functions of the R_{M-L} distances, studied using (top) basis 1 and (bottom) basis 2. The zero of energy was set at the lowest quintet minimum.

the metal−ligand interaction.[10] A full exploration of the PES ($3N - 6 = 147$ degrees of freedom in the LIESST compound) is unfortunately impossible. We have therefore defined a geometrical parameter Q that describes a continuous geometry change[11] from the LS structure (corresponding to $Q = -1$) to the HS high-temperature structure (where $Q = 1$). When $Q = 0$, the internal geometry is intermediate between those of the two states. It is worth noting that while this parameter introduces the variations of all of the angles and distances in the $[Fe(dipyrazolpyridine)_2]^{2+}$ complex of the $[Fe(dipyrazolpyridine)_2](BF_4)_2$ compound, it simply describes the variation of the coordination sphere radius R_{M-L} for $[Fe(NCH)_6]^{2+}$.

Section 2 is devoted to computational information, and the results are presented and analyzed in section 3. Finally, a more general discussion of the information obtained by such molecular studies of spin-transition compounds is presented in section 4, which is devoted to conclusions and perspectives.

2. Computational Aspects

This section presents both computational details and some results about the reliability of the approaches.

2.1. Computational Details. For the $[Fe(NCH)_6]^{2+}$ complex, distances between N, C, and H in the NCH ligand were kept

(5) Bolvin, H. *J. Phys. Chem. A* **1998**, *102*, 7525.
(6) Holland, J. M.; McAllister, J. A.; Lu, Z.; Kilner, C. A.; Thornton-Pett, M.; Halcrow, M. A. *Chem. Commun.* **2001**, 577.
(7) Holland, J. M.; McAllister, J. A.; Kilner, C. A.; Thornton-Pett, M.; Bridgemann, A. J.; Halcrow, M. A. *J. Chem. Soc., Dalton Trans.* **2002**, 548.
(8) Money, V. A.; Evans, I. R.; Halcrow, M. A.; Goeta, A. E.; Howard, J. A. K. *Chem. Commun.* **2003**, 158. Money, V. A.; Elhaïk, J.; Halcrow, M. A.; Howard, J. A. K. *Dalton Trans.* **2004**, 1516. Money, V. A.; Sánchez Costa, J.; Marcén, S.; Chastanet, G.; Elhaïk, J.; Halcrow, M. A.; Howard, J. A. K.; Létard, J. F. *Chem. Phys. Lett.* **2004**, *391*, 273. Thompson, A. L.; Money, V. A.; Goeta, A. E.; Howard, J. A. K. *C. R. Chim.* **2005**, *8*, 1365. Carbonera, C.; Sánchez, J.; Money, V. A.; Elhaïk, J.; Howard, J. A. K.; Halcrow, M. A.; Létard, J. F. *Dalton Trans.* **2006**, 3058. Elhaïk, J.; Kilner, C. A.; Halcrow, M. A. *Dalton Trans.* **2006**, 823. Carbonera, C.; Kilner, C. A.; Létard, J. F.; Halcrow, M. A. *Dalton Trans.* **2007**, 1284.
(9) Constant, G.; Daran, J. C.; Jeannin, Y. *C. R. Acad. Sci. Paris* **1967**, *265*, 808. Constant, G.; Daran, J. C.; Jeannin, Y. *J. Solid State Chem.* **1970**, *2*, 421. Constant, G.; Daran, J. C.; Jeannin, Y. *J. Inorg. Nucl. Chem.* **1973**, *55*, 493.
(10) Marchivie, M.; Guionneau, P.; Létard, J. F.; Chasseau, D. *Acta Crystallogr.* **2003**, *B59*, 479. Marchivie, M.; Guionneau, P.; Létard, J. F.; Chasseau, D. *Acta Crystallogr.* **2005**, *B61*, 25.
(11) Guihéry, N.; Malrieu, J.-P.; Maynau, D.; Handrick, K. *Int. J. Quantum Chem.* **1997**, *610*, 45.

fixed (the crystallographic value of R_{N-C} is 1.1 Å) as Q was varied. Distances and angles in the dipyrazolpyridine ligands were slightly modified such that the complex presents a C_{2v} symmetry point group. As will be shown, such changes did not affect the vertical spectra and are therefore not prejudicial to the study presented hereafter.

Calculations were performed using the complete active space second-order perturbation theory (CASPT2)[12] wave function-based method implemented in the MOLCAS 6.4 code.[13] This method treats nondynamic correlation variationally through the calculation of a multireference complete active space self-consistent field (CASSCF) zeroth-order wave function. Dynamic correlation is introduced in a second step by the perturbative treatment of the effect of single and double excitations on the previously calculated CASSCF wave function. CASSCF zeroth-order wave functions were computed using a double-shell active space containing the five 3d orbitals of the iron and five 3d′ orbitals dedicated to correlation. A previous work[14] has shown that this active space is adequate to reproduce the d−d transition energies.

For $[Fe(dipyrazolpyridine)_2]^{2+}$, model potentials including scalar relativistic effects were used to describe the 12 deep-core electrons of Fe and the $1s^2$ electrons of the N and C atoms. The corresponding optimized basis sets[15] (3s3p3d) for Fe, (2s3p1d) for N, (2s2p) for C, and 1s for H were used. A recent paper[16] has shown that the calculation of a converged energy difference between LS and HS ground states (computed in their own geometries) as a function of the basis set expansion requires the use of very large basis sets on both the metal and the ligand. Such large basis sets can hardly be used for the study of extended ligands. In order to validate the procedure, both the previous basis set, designated as basis 1, and a larger basis set, designated as basis 2, were used for the study of the $[Fe(NCH)_6]^{2+}$ complex. Basis 2 was constituted of all electron natural orbitals (ANO-RCC[20]), (5s4p3d2f1g) on Fe, (4s3p2d1f) on N and C, and (2s1p) on H (see ref 14 for a complete analysis of the basis set influence on the PEC).

2.2. Methodological Study of $[Fe(NCH)_6]^{2+}$. The spectra as functions of the R_{M-L} distances obtained using the two basis sets are presented in Figure 2. Since the O_h symmetry point group is not available in the MOLCAS code, the calculations were performed using the D_{2h} symmetry point group. The comparison of these spectra is very instructive. It shows the following:

• The two spectra are qualitatively similar, in particular with respect to (i) the locations of the crossings between the different states (R^c_{M-L}, values are reported in Table 1), which only slightly depend on the basis set, and (ii) the vertical transitions (reported in Figure 3), which are almost independent of the basis set at short distances.

• Since both the crossings and the vertical transitions are very similar in the two spectra, the main difference concerns the curvature of the states. In particular, the curvature of the singlet ground state is slightly more pronounced when the large basis set is used. As a consequence, the singlet minimum is stabilized by a non-negligible amount (0.35 eV) in comparison with the quintet one by the use of a larger basis set.

Table 1. Crossing Distances R^c_{M-L} between the Low-Energy States of the $[Fe(NCH)_6]^{2+}$ Complex Computed Using Basis 1 and Basis 2

	R^c_{M-L} (Å)	
states	basis 1	basis 2
$^1A_{1g}$, $^5T_{2g}$	1.975	1.963
$^1T_{1g}$, $^5T_{2g}$	1.800	1.805
$^1T_{1g}$, ^5E_g	2.017	2.025
$^1A_{1g}$, ^5E_g	2.124	2.107
$^1A_{1g}$, $^3T_{1g}$	2.120	2.078
^5E_g, $^3T_{1g}$	2.125	2.121
^5E_g, $^3T_{2g}$	2.072	2.088
$^1A_{1g}$, $^3T_{2g}$	2.240	2.141
$^5T_{2g}$, $^3T_{1g}$	1.886	1.881
$^5T_{2g}$, $^3T_{2g}$	1.832	1.838

Since one of the goals of this paper is to analyze the physical content of the low-energy states, we also compared the low-energy electronic wave functions calculated using the two basis sets. Both the nature of the molecular orbitals and the coefficients of the main reference (these states are essentially single-reference) do not depend on the basis set expansion. The difference in the coefficients never exceeds 2×10^{-3}, showing that the analysis of the physical content of these states can safely be done with the wave functions computed using basis 1.

2.3. Methodological Study of the $[Fe(dipyrazolpyridine)_2]^{2+}$ Complex of the $[Fe(dipyrazolpyridine)_2][BF_4]_2$ Compound. In order to validate the use of basis 1 for the study of $[Fe(dipyrazolpyridine)_2]^{2+}$, the electronic excitation from the quintet ground state in its experimental geometry to the first quintet excited state was computed. The obtained value of 1.20 eV compares very well with the available experimental value of 1.29 eV for a MeCN solution of the complex at 298 K.[7] This good agreement shows that the vertical spectrum is well-reproduced with this basis set, which means that the positions of the crossings between the different states are probably accurate as well. In order to measure the effect of the basis set expansion on the geometry in that peculiar complex, we optimized the geometry for both the quintet and singlet states using the B3LYP method (which gives the best agreement with

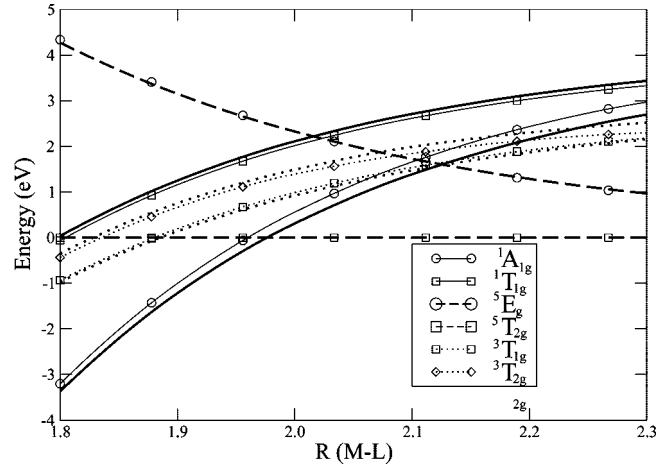

Figure 3. Vertical transition energies from the $^5T_{2g}$ ground state of the $[Fe(NCH)_6]^{2+}$ complex as functions of the R_{M-L} distances, studied using basis 1 (thin lines and symbols) and basis 2 (bold lines without symbols). Curves corresponding to the same transition obtained using the two basis sets are very close and even indistinguishable for quintet states.

(12) Andersson, K.; Malmqvist, P.-Å.; Roos, B. O.; Sadlej, A. J.; Wolinski, K. *J. Phys. Chem.* **1990**, *94*, 5483. Andersson, K.; Malmqvist, P.-Å.; Roos, B. O. *J. Chem. Phys.* **1992**, *96*, 1218.
(13) Karlström, G.; Lindh, R.; Malmqvist, P.-Å.; Roos, B. O.; Ryde, U.; Veryazov, V.; Widmark, P.-O.; Cossi, M.; Schimmelpfennig, B.; Neogradý, P.; Seijo, L. *Comput. Mater. Sci.* **2003**, *28*, 222.
(14) Képénékian, M.; Robert, V.; Le Guennic, B.; de Graaf, C. *J. Comput. Chem.*, submitted.
(15) Barandiaran, Z.; Seijo, L. *Can. J. Chem.* **1992**, *70*, 409.
(16) Pierloot, K.; Vancoillie, S. *J. Chem. Phys.* **2006**, *125*, 124303.
(17) Lawson Daku, L. M.; Vargas, A.; Hauser, A.; Fouqueau, A.; Casida, M. E. *ChemPhysChem* **2005**, *6*, 1393. Zein, S.; Matouzenko, G. S.; Borshch, S. A. *J. Phys. Chem. A* **2005**, *109*, 8568.

Table 2. Mean Fe−N Distances in the LS Singlet and HS Quintet Ground States in the $[Fe(dipyrazolpyridine)_2]^{2+}$ Complex Computed Using the B3LYP DFT Method with Different Basis Sets (with Experimental Data Included for Comparison)

	mean Fe−N distance (Å)	
basis set	LS state	HS state
STO-3G	1.857	2.089
6-31G	1.967	2.175
AugccpVTZ	1.993	2.203
experimental[a]	1.953	2.165

[a] Data from ref 7.

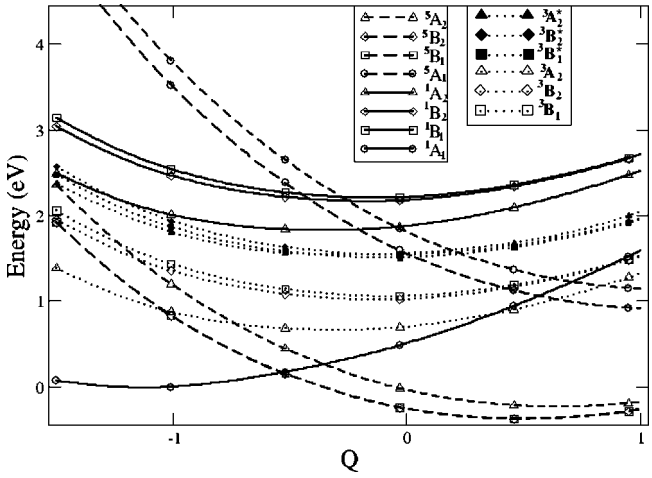

Figure 4. Spectrum of the $[Fe(dipyrazolpyridine)_2]^{2+}$ complex as a function of the coordinate Q that changes both the R_{M-L} distances and the ligand distortions. The curves corresponding to the lowest quintet states $^5B_1$ and $^5B_2$ are almost undistinguishable.

experiment[17]) with several different basis sets. The mean Fe−N distances obtained are reported in Table 2. A comparison of these values shows that the geometry is strongly dependent on the basis set expansion when the B3LYP DFT method is used (as recently reported in ref 18). The mean Fe−N distance increases with the basis set expansion. Part of the error may be attributed to basis set superposition error. The counterpoise method has been used to correct this defect in the PECs computed at the CASPT2 level using basis 1 and an ionization potential electron affinity (IPEA) shift of 0.5. The PECs so obtained are shown in Figure 4. Whereas without the counterpoise correction the mean Fe−N distances are smaller than the experimental ones (1.895 Å for the singlet and 2.06 Å for the quintet), the corrected well minima are quite close to the experimental ones, but the quintet state has the lowest minimum ($\Delta E_{HS} = 0.37$ eV and $E^{quintet}_{Q=1} - E^{singlet}_{Q=-1} = 0.27$ eV). As already shown in ref 16 and confirmed in the present study of $Fe(NCH)_6]^{2+}$, the ground-state singlet energy is underestimated unless very large basis sets are used. A stabilization of 0.35 eV with respect to the quintet state was obtained for the previous complex when using basis 2. A stabilization of the same order of magnitude would restore the singlet as the lowest minimum in the $[Fe(dipyrazolpyridine)_2]^{2+}$ complex.

Moreover, the energy differences between states at different geometries are probably more sensitive to the environment of the molecule in the material than to the basis sets, in particular for cooperative systems. As shown in ref 7, the nature of the ground state may change according to the counterion (either BF_4^- or PF_6^-). The main effect of the nature of the counterion that affects the geometrical structure of the complex was taken into account in our calculations (crystallographic structures were considered). Nevertheless, in the HS structure, the ligand−BF_4^- distances are slightly reduced. Indeed, the mean distance between the N(pyridine) of a ligand and the B atoms of the two closest counterions is ∼4.45 Å in the HS structure and ∼4.63 Å in the LS one. Thus, larger electrostatic and Pauli exclusion repulsions between the negative charges of the counterions and the electrons of the ligand π systems are expected. As a consequence, the effect of the counterions should be a relative destabilization of the quintet well minima. Most of the experimental features also depend on the phases (either liquid or solid) and on the solvent in the liquid phase. For these reasons, the calculation of a precise adiabatic spectrum of the isolated complex is beyond the scope of the present study.

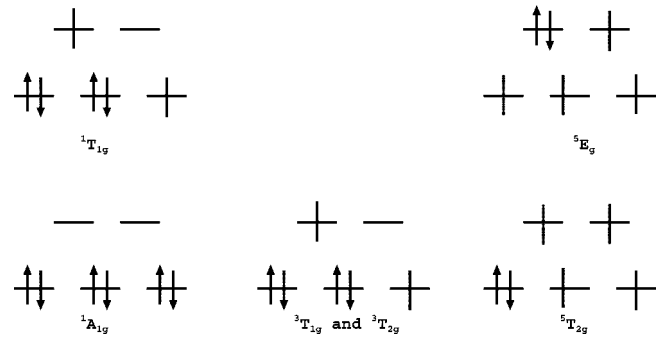

Figure 5. Dominant spatial configurations of the singlet, triplet, and quintet states of the octahedral $[Fe(NCH)_6]^{2+}$ complex.

In any event, one should note that the electrostatic effects of the BF_4^- counterions (modeled as point charges) only slightly affect the computed vertical transition energies (2.75% on the singlet−quintet transition energy of the LS phase), so our calculations should provide a realistic description of the different states. Thus, we will now turn our attention to the analysis of the different wave functions and a qualitatively discussion of the different crossings of the states that could be involved in both the LIESST and reverse LIESST mechanisms.

3. Qualitative Analysis of the Spectra and the Corresponding Wave Functions

3.1. The $[Fe(NCH)_6]^{2+}$ Complex. Because of the high symmetry (O_h) of the $[Fe(NCH)_6]^{2+}$ complex, most of the states are degenerate (see Figure 2). The represented spectrum consists of a orbitally threefold-degenerate quintet ground state ($^5T_{2g}$), one closed-shell singlet ground state ($^1A_{1g}$), one orbitally threefold-degenerate excited singlet ($^1T_{1g}$), two orbitally threefold-degenerate triplets ($^3T_{1g}$ and $^3T_{2g}$), and a orbitally twofold-degenerate excited quintet (^5E_g). The dominant spatial configurations of these states are represented in Figure 5. The relative positions of the well minima can be rationalized by looking at the occupation number of the e_g orbitals in the different states. As shown in Figure 2, the $^1A_{1g}$ ground state, which has zero electrons in the e_g σ antibonding orbitals, has the smallest coordination sphere (at $Q = -1$, $R_{M-L} = 1.95$ Å). The excited T_{1g} and T_{2g} singlet and triplet states, each of which has a single electron in the e_g orbitals, have coordination sphere radii of 2.06 Å. The $^5T_{2g}$ ground state has two electrons in the e_g orbitals, and its coordination sphere radius is $R_{M-L} = 2.15$ Å (which compares very well with the crystallographic value, $R_{M-L} =$

(18) Güell, M.; Luis, J. M.; Solà, M.; Swart, M. *J. Phys. Chem A* **2008**, *112*, 6384.

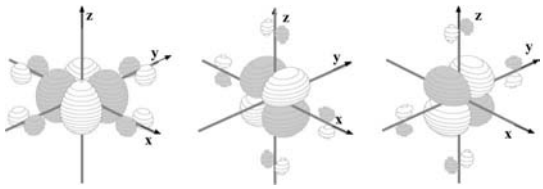

Figure 6. The t_{2g} molecular orbitals of the octahedral $[Fe(NCH)_6]^{2+}$ complex. The NCH ligands are located on the axes.

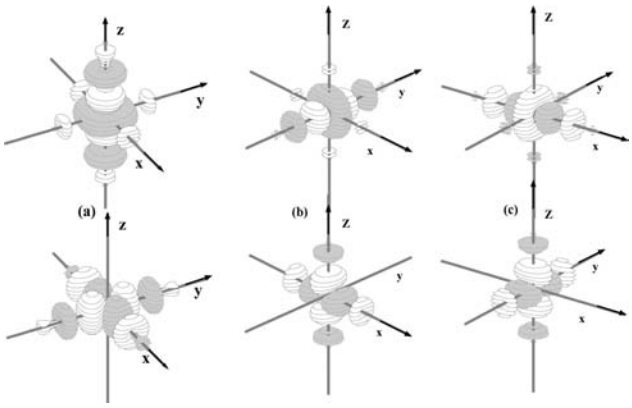

Figure 7. The e_g molecular orbitals of the octahedral $[Fe(NCH)_6]^{2+}$ complex: (a) $d_{x^2-y^2}$ (bottom) and d_{z^2} (top); (b) $d_{x^2-z^2}$ (bottom) and d_{y^2} (top); (c) $d_{y^2-z^2}$ (bottom) and d_{x^2} (top).

2.16 Å[9]). Finally, the excited ^5E_g state, which has three electrons in the e_g orbitals, has the largest coordination sphere (R_{M-L} = 2.25 Å).

The studied states are dominated by a single configuration when three different orbital sets are used. The nature of the t_{2g} orbitals (Figure 6) is common to all of the sets, while the e_g orbitals have various orientations and can be described as either (d_{z^2}, $d_{x^2-y^2}$), (d_{y^2}, $d_{x^2-z^2}$) or (d_{x^2}, $d_{y^2-z^2}$) (Figure 7). The different sets of e_g orbitals can be obtained by simple rotation from one set to another. The energy differences between the spatial configurations (and therefore between the different states) have been quantified using Racah coefficients.[19] However, in order to understand the different qualitative features between the spectra of the ideal octahedral system $[Fe(NCH)_6]^{2+}$ and the distorted (from the octahedral symmetry) $[Fe(dipyrazolpyridine)_2]^{2+}$ complex, in particular along the Q coordinate, an analysis of the different wave functions and a short presentation of the main electrostatic arguments will be helpful.

First, in the closed-shell $^1A_{1g}$ state and the ^5E_g state, the t_{2g} orbitals have the same occupation number (2 and 1, respectively). The electron repulsion between the d electrons is equivalent whatever the nature of the e_g orbitals.

On the contrary, in the $^1T_{1g}$, $^3T_{1g}$, and $^3T_{2g}$ states, the t_{2g} orbitals have different occupation numbers. The T_{1g} spatial configurations have lower energy than the T_{2g} ones, and the electron repulsion of the d electrons differs according to the nature of the filled e_g orbital. In the lowest-energy states, $^3T_{1g}$ and $^1T_{1g}$, the nature of the filled e_g orbital is either $d_{x^2-y^2}$, $d_{y^2-z^2}$, or $d_{x^2-z^2}$, depending on the nature of the singly occupied t_{2g} orbital (either d_{xy}, d_{yz}, or d_{xz}, respectively). For instance, in the d-orbital spatial configuration

$$(T_{1g}) = (d_{yz})^2(d_{xy})^2(d_{xz})(d_{x^2-z^2}) \quad (1)$$

(19) Griffith, J. S. *The Theory of Transition Metal Ions*; Cambridge University Press: Cambridge, U.K., 1964.

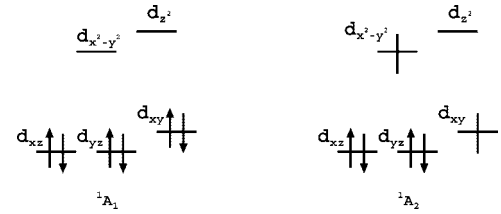

Figure 8. Dominant spatial configurations of the two lowest singlet states in the $[Fe(dipyrazolpyridine)_2]^{2+}$ complex.

four electrons occupy the t_{2g} orbitals spread over the y axis. The spatial configuration that minimizes the electron repulsion is therefore the one in which a $d_{x^2-z^2}$ orbital, which does not contain any component in the y direction, is preferencially filled. As a consequence, the higher-energy T_{2g} states are dominated by spatial configurations in which either the d_{x^2}, d_{y^2}, or d_{z^2} orbital is filled. For instance, the dominant spatial configuration of the T_{2g} state in which the d_{xz} orbital is singly occupied is

$$(T_{2g}) = (d_{yz})^2(d_{xy})^2(d_{xz})(d_{y^2}) \quad (2)$$

The energy difference between the (T_{1g}) and (T_{2g}) spatial configurations is given by

$$E(T_{1g}) - E(T_{2g}) = 2J_{(x^2-z^2)(yz)} + 2J_{(x^2-z^2)(xy)} + J_{(x^2-z^2)(xz)} - 2J_{(y^2)(yz)} - 2J_{(y^2)(xy)} - J_{(y^2)(xz)} \quad (3)$$

where $J_{(a)(b)}$ indicates the Coulomb repulsion integral between an electron in orbital a and an electron in orbital b. Of course, for symmetry reasons, the other (T_{1g}) and (T_{2g}) spatial configurations obtained by interchanging the x, y, or z component in eq 3 are strictly identical. Moreover, because of the high symmetry of the complex, the tails of the magnetic orbitals on the ligand are similar in all directions, and this energy difference slightly depends on the R_{M-L} distances. As a consequence, the PECs of the $^3T_{1g}$ and $^3T_{2g}$ states are almost parallel over the whole range of interesting R_{M-L} distances (i.e., around their well minima).

Finally, one should note as well the parallelism of PECs for the $^1T_{1g}$ and $^3T_{1g}$ states. Since the spatial parts of these wave functions are identical, they differ only in their spin multiplicities. Their energetic ordering is therefore governed by the Hund's rule, and their energy difference ($\Delta E_{ST} = 2K$) is proportional to the atomic exchange integral K between d orbitals, which is also quite insensitive to the R_{M-L} distances.

For the two last reasons, no crossing between the $^1T_{1g}$ and $^3T_{2g}$ states in an octahedral complex would be expected, if the considered Q coordinate is restricted to the R_{M-L} distance.

3.2. The $[Fe(dipyrazolpyridine)_2]^{2+}$ Complex of the $[Fe(dipyrazolpyridine)_2](BF_4)_2$ Compound. Because of the ligand geometrical constraints imposed by the coordination sphere increase along the Q coordinate, the distances between the Fe ion and the nearest-neighbor N atoms in this complex differ (~1.90, ~1.97, and ~1.99 Å in the LS phase and ~2.13, ~2.18, and ~2.20 Å in the HS phase). The N−Fe−N angles are also not identical and vary along the Q coordinate. This distortion from the octahedral symmetry leads to a removal of degeneracy in all of the states. The leading spatial configurations of the different wave functions are shown in Figures 8 and 9. The calculated spectrum (see Figure 4) presents the following features:

• As in the previous complex, the positions of the well minima in the PECs of the lowest states are still governed by the occupation of the e_g orbitals.

• The energies of the lowest quintet states in this complex are split into three different values, the two lowest ones still being almost degenerate (ΔE = 3.5 meV for Q = 1).

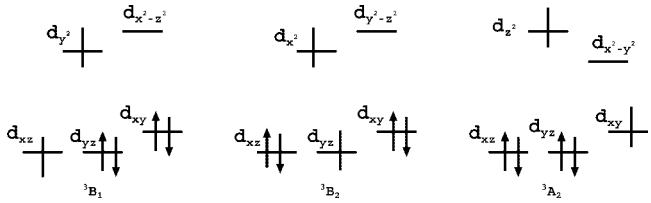

Figure 9. Dominant configurations of the three lowest triplet states in the $[Fe(dipyrazolpyridine)_2]^{2+}$ complex.

• The main changes with respect to the spectrum obtained in octahedral symmetry concern the excited singlet and triplet states. The $^3T_{1g}$ state from the octahedral case here is split into two sets of states, the $^3A_2$ state, which is lowest in energy, and the $^3B_1$ and $^3B_2$ states, which are highest in energy and almost degenerate. The removal of the degeneracy of the states issuing from $^3T_{2g}$ leads to the three higher-energy states $^3A_2^*$, $^3B_1^*$ and $^3B_2^*$. The most significant qualitative difference between this spectrum and the previous one is the occurrence of crossings between the lowest $^1A_2$ state and several excited triplet states in the Franck−Condon region. These triplets are now more likely to participate in the LIESST mechanism.

• The PECs of the singlet states issuing from $^1T_{1g}$ are almost parallel to those of the triplet states with corresponding symmetries issuing from $^3T_{1g}$ (those of the three highest singlet states issued from $^1T_{2g}$ were not computed). As already explained in the octahedral case, their energy difference is still governed by the atomic exchange integral K of the iron ion.

This different energetic ordering of the states can be rationalized by considering their main spatial configuration, the orientation of the e_g orbitals, and electrostatic arguments. As in the octahedral case, the states are essentially single-reference in their optimized set of orbitals, and their physical content is rather similar to that of the states of the octahedral case from which they issued.

The t_{2g}-like orbitals of all of the states are d_{xz} of irreducible representation (irrep) B_1, d_{yz} of irrep B_2, and d_{xy} of irrep A_2 in the C_{2v} symmetry point group. The e_g-like orbitals are of d_{z^2} and $d_{x^2-y^2}$ nature for the A_1 and A_2 states, d_{x^2} and $d_{y^2-z^2}$ nature for the B_1 states, and d_{y^2} and $d_{x^2-z^2}$ nature for the B_2 states. The e_g-like orbitals of irrep A_1 optimized for the triplet states of symmetry B_1, B_2, and A_2 are represented in Figure 10.

It is worth noting that contrary to the octahedral case, the different sets of orbitals can no longer be obtained from each other by simple rotations. Indeed, because of the geometrical distortion, the strength of the ligand field is now different in the three directions. The orbitals optimized for states of different symmetries have not only a different orientation but also different tails on the ligands. As a consequence, the Coulomb repulsion integrals are different for all of the orbital pairs, and the energy differences between the states of different symmetries are no longer identical upon interchange of the x, y, or z component in eq 3. Moreover, the expectation values of the monoelectronic operator of the Hamiltonian are different for each different spatial distribution. In any distorted complex, the PECs of the states issuing from the T_{2g} and T_{1g} states can be more or less repulsive according to the orientation and nature of the filled orbitals and have no reason to be parallel. The distortion is therefore responsible for the occurrence of a crossing between the triplet states issuing from $^3T_{2g}$ and one of the singlet states issuing from $^1T_{1g}$.

In the complex studied in this work, two peculiar features of the distorted ligand field rationalize the obtained splitting of the states:

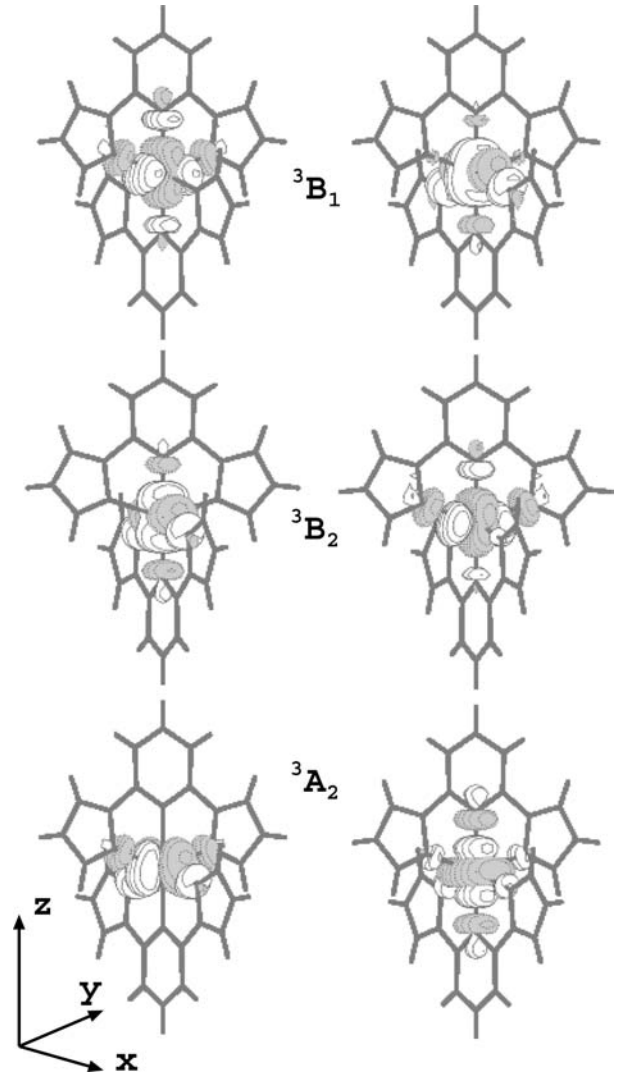

Figure 10. Selected e_g-like molecular orbitals of the $[Fe(dipyrazolpyridine)_2]^{2+}$ complex.

• The energetic ordering of the t_{2g}-like orbitals is unexpected because the shortest Fe−N distances are along the z axis, which should in principle lead to a destabilization of the d_{xz} and d_{yz} orbitals relative to the d_{xy} orbital. The orbital occupation of the two lowest-energy, almost degenerate $^5B_1$ and $^5B_2$ states shows that the $a_2 = d_{xy}$ orbital is always half-filled for these states, while it is doubly occupied in the higher-energy $^5A_2$ state (issued from the $^5T_{2g}$ ground state as well). This confirms that in a monoelectronic picture, this orbital may be seen as having a higher energy than the almost degenerate d_{xz} and d_{yz} orbitals. Actually, as already shown in a previous DFT study,[7] the overlap of this orbital with the π systems of the two dipyrazolpyridine ligands is responsible for its larger antibonding character. In spatial configurations with two unpaired electrons, this a_2 orbital is half-filled for those of the A_2 irrep but doubly occupied for those of the B_1 and B_2 irreps. This feature is responsible for the lower energetic positions of both the $^1A_2$ and $^3A_2$ states issuing from T_{1g} states relative to the corresponding singlet and triplet B_1 and B_2 states.

• The energetic ordering of the e_g-like orbitals is as expected for a slightly distorted octahedral structure in which the ligand field along z is stronger. Indeed, as observed experimentally, the two E_g-like quintet states ($^5A_1$), which differ in the occupation of the d_{z^2} and $d_{x^2-y^2}$ orbitals, are split by ∼0.3 eV.

Consistently, the $^3A_2^*$ state is not lower in energy than the $^3B_1^*$ and $^3B_2^*$ states issuing from the $^3T_{2g}$ state, while here again the d_{xy} orbital is half-filled. Actually, the e_g-like orbital that is filled in this state is the d_{z^2} orbital, which is the most antibonding one (in comparison with d_{x^2} and d_{y^2}, which are filled in the two other states). These two factors compensate for each other, and the PECs of the three states issuing from the $^3T_{2g}$ state are slightly split.

4. Discussion

The analysis of spectra and wave functions of two complexes has been performed in a wave function-based ab initio study. The obtained results provide a rationalization of several qualitative features of spin transition compounds, which are described in the following paragraphs.

The positions of the well minima in all of the interesting states are governed by the number of e_g electrons. This feature imposes a common shape to the spectra of all of the spin-transition compounds. The Fe−N distances for the triplet state wells are expected to be halfway between those of the lowest singlet and quintet wells (this corresponds to case 1 of ref 21), which facilitates the spin crossover. In particular, the well minima of the excited singlet and triplet states having a single e_g electron are located at the same value of the coordination sphere radius.

The interaction of the d_{xy} orbital of the metal center with the π system of the ligands in the $[Fe(dipyrazolpyridine)_2]^{2+}$ complex is responsible for the removal of the quintet ground state degeneracy, with the two quintet states remaining quasi-degenerate. Such a situation is likely to occur in many spin-transition compounds. The main consequence of this quasi-degeneracy concerns the entropy calculation, which in most studies is performed only for one quintet state and is therefore underestimated. It is worth noting that for an octahedral complex, this degeneracy is triple.

Simple electrostatic arguments rationalize the energetic order of the different spatial configurations and therefore of the different states. The orientation of the e_g-like orbitals depends on the occupation numbers of the t_{2g}-like orbitals, and the energy difference between the two sets of triplet (and singlet) states that could be involved in the LIESST mechanism depends on the Coulomb repulsion integrals between the d electrons.

The energetic ordering of the states having the same spatial configuration follows Hund's rule, and their energy difference is proportional to the metal exchange integral between the d orbitals.

As a consequence of the previous points, in a strictly octahedral geometry, the singlet and triplet curves are almost parallel in the Franck−Condon region, and no crossing between these states occurs. A relaxation process from the excited singlet through any triplet state therefore appears quite unlikely.

On the contrary, distortions from the octahedral symmetry result in a removal of degeneracy of the triplet states, leading to a crossing between the lowest excited singlet and several triplets in the Franck−Condon region. Several channels may be proposed for both the LIESST (see Figures 11, 12, and 13) and the reverse LIESST (see Figure 14) mechanisms. Let us start by the relaxation processes consecutive to the $^1A_1$-$^1A_2$ absorption:

• A four-step pathway (see Figure 11): $^1A_2 \rightarrow {}^3T_{2g}$-like (excited $^3B_1$, $^3B_2$, or $^3A_2$) $\rightarrow {}^5E_g$-like ($^5A_1$) $\rightarrow {}^3T_{1g}$-like (lowest $^3A_2$) $\rightarrow {}^5T_{2g}$-like ground state ($^5B_1$ or $^5B_2$). From the excited singlet state, a first relaxation should bring the system into one of the $^3T_{2g}$-like states. A conical intersection between these states and the $^3T_{1g}$-like ones is not expected because of the low dependence of the energy difference between these states on the geometry of the complex (see eq 3). Nevertheless, the $^3T_{2g} \rightarrow {}^3T_{1g}$ transition can be mediated by a first relaxation to the excited ^5E_g-like state that crosses both PECs. Finally, a $^3T_{1g} \rightarrow$

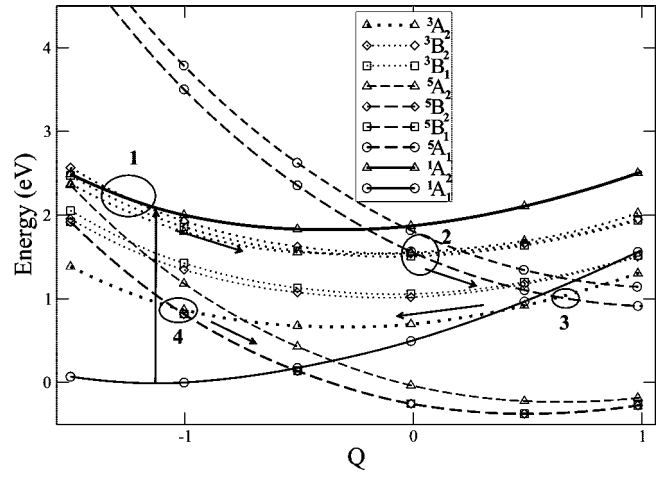

Figure 11. A four-step LIESST mechanism: $^1A_2 \rightarrow$ excited $^3B_1$, $^3B_2$, or $^3A_2 \rightarrow {}^5A_1 \rightarrow$ lowest $^3B_1$, $^3B_2$, or $^3A_2 \rightarrow {}^5B_1$ or $^5B_2$. Labels 1, 2, 3, and 4 indicate the first, second, third, and fourth crossings (see text).

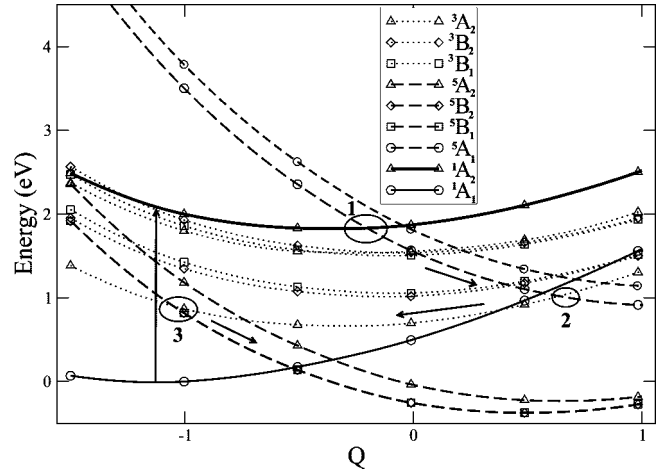

Figure 12. A three-step LIESST mechanism: $^1A_2 \rightarrow {}^5A_1 \rightarrow$ lowest $^3B_1$, $^3B_2$, or $^3A_2 \rightarrow {}^5B_1$ or $^5B_2$. Lables 1, 2, and 3 indicate the first, second, and third crossings (see text).

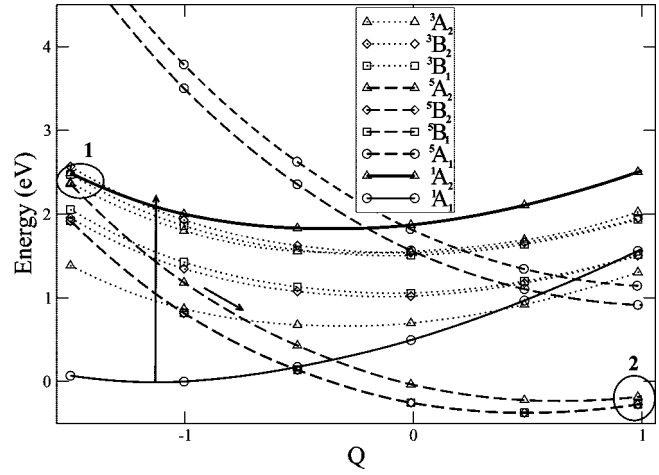

Figure 13. A two-step LIESST mechanism: $^1A_2 \rightarrow {}^5A_2 \rightarrow {}^5B_1$ or $^5B_2$. Labels 1 and 2 indicate the first and second crossings.

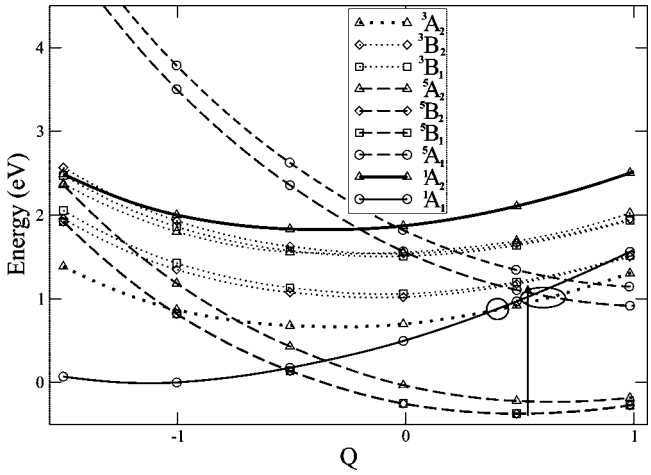

Figure 14. Two channels for the reverse LIESST mechanism: a two-step pathway ($^5A_1 \rightarrow {}^3A_2 \rightarrow {}^1A_1$) and a one-step pathway ($^5A_1 \rightarrow {}^1A_1$).

$^5B_1$ or $^3T_{1g} \rightarrow {}^5B_2$ transition would complete the LIESST mechanism. An alternative pathway for the last transition would be a $^3T_{1g} \rightarrow {}^5A_2$ crossing followed by an intramolecular vibrational redistribution to the lowest quintet states.

• A three-step pathway (see Figure 12): $^1A_2 \rightarrow {}^5E_g$-like ($^5A_1$) $\rightarrow {}^3T_{1g}$-like (lowest $^3B_1$, $^3B_2$, or $^3A_2$) $\rightarrow {}^5T_{2g}$-like ground state ($^5B_1$ or $^5B_2$). From the excited singlet state, a direct relaxation to the excited ^5E_g-like state leads to a shorter pathway. It is worth noting that the spin−orbit coupling between singlet and quintet states is expected to be much smaller than that between singlet and triplet or triplet and quintet states. As in the previous LIESST mechanism, the same alternative pathway for the last transition could be followed.

• A two-step pathway (see Figure 13): $^1A_2 \rightarrow$ excited $^5T_{2g}$-like ($^5A_2$) $\rightarrow {}^5T_{2g}$-like ground state ($^5B_1$ or $^5B_2$). The distortion from the octahedral symmetry lifts the degeneracy of the $^5T_{2g}$-like states and leads to a crossing between the highest $^5T_{2g}$-like state and the excited $^1A_2$ states in the Franck−Condon region. Also, such a pathway involves spin−orbit coupling between a singlet and a quintet state. However, the second step [$^5T_{2g}$-like ($^5A_2$) $\rightarrow {}^5T_{2g}$-like ($^5B_1$ or $^5B_2$)] is expected to be very fast.

• A non-LIESST two-step pathway: $^1A_2 \rightarrow {}^3T_{2g}$-like (excited $^3B_1$, $^3B_2$, or $^3A_2$) $\rightarrow {}^1A_1$. One should note that the singlet ground state PEC crosses the $^3T_{2g}$-like PEC at large distances, inducing an efficient relaxation back to the singlet ground state. The efficiency of this channel relative to the LIESST pathways rationalizes the necessity of a long pumping irradiation to populate the HS state.

With respect to the reverse LIESST mechanism, two channels may be envisaged as well: a two-step pathway (^5E_g-like $\rightarrow {}^3T_{1g}$-like $\rightarrow {}^1A_1$) and a one-step pathway (^5E_g-like $\rightarrow {}^1A_1$) (see Figure 14). Indeed, the PEC of the quintet excited state crosses the PECs of both the lowest triplet state and the singlet ground state. Here again, the competition between the one-step and two-step mechanisms of relaxation depends on the spin−orbit couplings of the differents states.

It should be noticed that, in all of the mechanisms involving the ^5E_g-like state, the two nearly degenerate $^5A_1$ states are likely to play a similar role, increasing the efficiency of the concerned pathways.

To summarize our suggestions, which keep a speculative character, the proposed pathways involve either a large number of transitions between first-order-coupled spin−orbit states (singlet−triplet and triplet−quintet) or a smaller number of transitions between weakly coupled states (singlet−quintet). However, the relaxation processes of both the LIESST and reverse LIESST mechanisms are known to be very fast.[22] Thus, in order to determine which of the proposed pathways is preferred, a dynamical study is compulsory. Such a study requires the evaluation of the spin−orbit couplings between the different states. This will be the subject of a forthcoming paper.

A theoretical study of a Fe(III) LIESST compound[21] has shown the possible role of ligand-to-metal electron transfer excitation in initiating LIESST and reverse LIESST. This point deserves further examination, but we should remark that in the complex studied in our work, for the HS geometry, the lowest excited quintet state does not have ligand-to-metal electron transfer character, and the corresponding transition energy agrees with the experimental value.

Finally, this study has analyzed the possible nonradiative processes of deexcitation within the d−d states. One cannot exclude a possible participation of the ligand in the relaxation process.[23] Since distortions from the octahedral symmetry play a crucial role, a refined exploration of the potential energy surfaces in the Franck−Condon region, including the localization of conical intersections, would be welcome. More experimental studies would be helpful to further orient theoretical studies to elucidate these intriguing mechanisms.

Acknowledgment. This paper is dedicated to the memory of Jean-Pierre Daudey. We kindly thank Dr. G. Molnár and Dr. A. Bousseksou for helpful discussions. Dr. J.-P. Malrieu, Dr. M. C. Heitz, Dr. M. Boggio-Pasqua, and Dr. N. Halberstadt are also acknowledged. Most of the calculations were performed at the IDRIS center under Project 1104. DFT calculations were performed at CICT (Toulouse). This work was supported by the French Centre National de la Recherche Scientifique (CNRS), the Université de Toulouse, and the GDR Magnétisme et Commutation Moléculaire.

Supporting Information Available: Fe−N distances, low-energy spectra, and Z matrices for the well minima of the singlet $^1A_1$ and quintet $^5B_1$ and $^5B_2$ (identical minima) states. This material is available free of charge via the Internet at http://pubs.acs.org.

JA805626S

(20) Widmark, P.-O.; Malmqvist, P.-Å.; Roos, B. O. *Theor. Chim. Acta* **1990**, *77*, 291. Roos, B. O.; Lindh, R.; Malmqvist, P.-Å.; Veryazov, V.; Widmark, P.-O. *J. Phys. Chem. A* **2004**, *108*, 2851. Roos, B. O.; Lindh, R.; Malmqvist, P.; Veryazov, V.; Widmark, P.-O. *J. Phys. Chem. A* **2005**, *109*, 6575.

(21) Ando, H.; Nakao, Y.; Sato, H.; Sakaki, S. *J. Phys. Chem. A* **2007**, *111*, 5515.

(22) Hauser, A. *J. Chem. Phys.* **1991**, *94*, 2741. Buron-Le, M.; Collet, E.; Guérin, L.; Lemée-Cailleau, M. H.; Cailleau, H.; Wulff, M.; Luty, T.; Koshihara, S.; Tanaka, K. *J. Lumin.* **2005**, *112*, 235. Gawelda, W.; Pham, V.-T.; Benfatto, M.; Zaushitsyn, Y.; Kaiser, M.; Grolimund, D.; Johnson, S. L.; Abela, R.; Hauser, A.; Bressler, Ch.; Chergui, M. *Phys. Rev. Lett.* **2007**, *98*, 057401. Gawelda, W.; Cannizzo, A.; Pham, V.-T.; van Mourik, F.; Bressler, C.; Chergui, M. *J. Am. Chem. Soc.* **2007**, *129*, 8199. Krivokapic, I.; Enachescu, C.; Bronisz, R.; Hauser, A. *Chem. Phys. Lett.* **2008**, *455*, 192.

(23) Lawthers, I.; McGarvey, J. J. *J. Am. Chem. Soc.* **1984**, *106*, 4280. Roux, C.; Zarembowitch, J.; Gallois, B.; Granier, T.; Claude, R. *Inorg. Chem.* **1994**, *33*, 2273. Boillot, M. L.; Chantraine, S.; Zarembowitch, J.; Lallemand, J. Y.; Prunet, J. *New J. Chem.* **1999**, *23*, 179. Halcrow, M. A. *Polyhedron* **2007**, *26*, 3523.